

## Electrical conduction in the $\text{Si}(111)\text{:B-}(\sqrt{3}\times\sqrt{3})R\ 30^\circ/a\text{-Si}$ interface reconstruction

R. L. Headrick, A. F. J. Levi, H. S. Luftman, J. Kovalchick, and L. C. Feldman  
*AT&T Bell Laboratories, Murray Hill, New Jersey 07974*

(Received 13 July 1990)

One-third of a monolayer of spatially ordered boron on (111)-oriented crystalline silicon is prepared in ultrahigh vacuum and then buried under a thin layer of amorphous silicon. This leaves a two-dimensional  $(\sqrt{3}\times\sqrt{3})$  boron layer in substitutional sites confined to a single monolayer on the crystalline side of the interface. We report electrical conductivity with a high  $p$ -type carrier density ( $> 10^{14}/\text{cm}^2$ ) in an ordered two-dimensional interface layer.

We have recently shown that a stable derivative of the  $\text{Si}(111)\text{:B-}(\sqrt{3}\times\sqrt{3})R\ 30^\circ$  surface structure can be created by capping the surface with amorphous silicon.<sup>1</sup> In this paper we investigate the electrical properties of the  $\text{Si}(111)\text{:B-}(\sqrt{3}\times\sqrt{3})R\ 30^\circ/a\text{-Si}$  two-dimensional ordered phase. Although tunneling spectroscopy and first-principles calculations<sup>2,3</sup> show that the  $\text{B-}(\sqrt{3}\times\sqrt{3})R\ 30^\circ$  surface is semiconducting with a band-gap comparable to that of bulk silicon, we find that the  $\text{B-}(\sqrt{3}\times\sqrt{3})R\ 30^\circ/a\text{-Si}$  interface structure is conducting at low temperature (i.e., it is a two-dimensional metal). To our knowledge, this is the first report of electrical activity associated with an *ordered, two-dimensional impurity layer* in a semiconductor. We attribute the activation of free carriers at the  $\text{B-}(\sqrt{3}\times\sqrt{3})R\ 30^\circ/a\text{-Si}$  interface to passivation of surface dangling bonds by the amorphous-silicon layer. The existence of the electrically active ordered impurity layer establishes this example as the ultimate in silicon  $\delta$ -doping since the impurity layer is confined to a single monolayer.

The  $\text{Si}(111)\text{B-}(\sqrt{3}\times\sqrt{3})R\ 30^\circ$  surface consists of an array of Si adatoms in  $T_4$  sites atop the surface and one boron atom per primitive unit cell of the reconstruction occupying ordered lattice sites.<sup>1-3</sup> This corresponds to a boron coverage of  $\frac{1}{3}$  monolayer, or  $4/\sqrt{27}a^{-2}=2.6\times 10^{14}\text{ cm}^{-2}$ , where  $a$  is the lattice parameter of silicon. Figure 1 shows the  $\text{Si}(111)\text{:B-}(\sqrt{3}\times\sqrt{3})R\ 30^\circ/a\text{-Si}$  interface reconstruction. The interface is a simple modification of the surface structure in which the silicon adatoms in  $T_4$  sites are displaced from ordered sites and become part of the amorphous overlayer.<sup>1,4,5</sup> X-ray-diffraction measurements show that the first complete layer of the silicon crystal remains ordered, as does the layer in which boron is substituted.<sup>1</sup> The capped reconstruction is stable in air indefinitely, and heating to less than  $150^\circ\text{C}$  produces no noticeable degradation of the interface as measured by x-ray diffraction.<sup>4</sup>

Samples were prepared in a molecular-beam epitaxy chamber equipped with an electron gun evaporator to deposit silicon, a quartz-crystal thickness monitor, and a Knudsen cell to deposit boron from  $\text{HBO}_2$ . The samples were cut from a wafer of  $8\ \Omega\text{ cm}$   $n$ -type (arsenic)  $\text{Si}(111)$ . The surfaces were prepared by chemical growth of a thin protective oxide layer. Once in the vacuum system the oxide on each sample was reduced with a Si beam while

the sample was held at  $700^\circ\text{C}$ .<sup>6</sup> Boron was then deposited onto the surface for 3 min, and the sample was cooled to room temperature. Low-energy electron diffraction (LEED) and Auger-electron spectroscopy (AES) were performed *in situ* to confirm that a sharp  $\sqrt{3}\times\sqrt{3}$  LEED pattern was obtained and that the boron coverage had reached saturation ( $\frac{1}{3}$  monolayer). The sample was then covered with 20–350 Å of amorphous silicon. The 178-eV boron Auger signal decreased exponentially as a function of  $a\text{-Si}$  thickness with a decay constant equal to the inelastic mean free path<sup>7</sup> of 178-eV electrons through amorphous silicon. This confirms that boron is buried without surface segregation during the  $a\text{-Si}$  deposition. Control samples that were prepared without intentional boron exhibited a  $7\times 7$  LEED pattern; the  $7\times 7$  reconstruction is also known to remain ordered after capping with  $a\text{-Si}$ .<sup>8,9</sup>

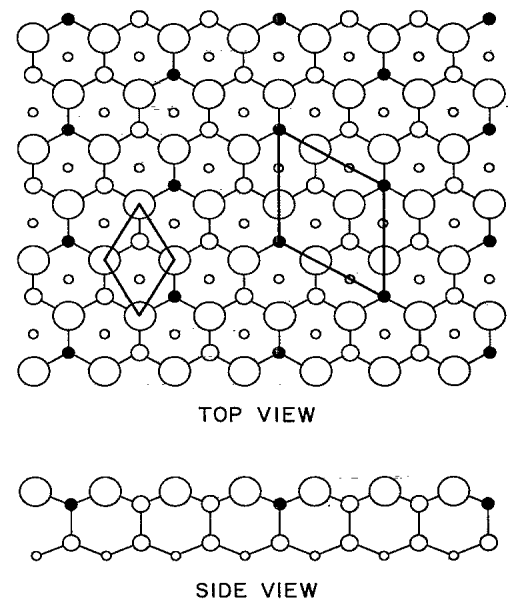


FIG. 1. The  $\text{Si}(111)\text{:B-}(\sqrt{3}\times\sqrt{3})R\ 30^\circ/a\text{-Si}$  interface reconstruction. Silicon is represented as open circles with varying sizes to show depth; boron is represented as solid circles. An amorphous-silicon layer (not shown) covers the ordered structure.

X-ray-diffraction, secondary-ion mass spectroscopy, nuclear reaction analysis, and low-temperature Hall-effect measurements were performed after removing the  $a$ -Si capped samples from the vacuum system. The purposes of these probes are, respectively, (1) to assure the maintenance of the ordered boron layer, (2) to search for possible boron diffusion, (3) to provide an absolute and independent calibration of the boron content, and (4) to characterize the electrical properties of the system. The x-ray-diffraction equipment was a four-circle diffractometer with a Cu  $K\alpha$  rotating anode source and graphite monochromator. Secondary-ion mass spectroscopy (SIMS) was performed using a Phi model 660 system using a 3-keV  $O_2^+$  beam and a quadrupole analyzer.

The absolute boron coverage was obtained by nuclear reaction analysis (NRA) using 650-keV protons and the  $^{11}B(p,\alpha)^8Be$  reaction.<sup>10</sup> The concentration of boron was calibrated by comparison with a silicon standard that was implanted with a known amount of  $^{11}B$ . Bridge geometry mesas were defined on the samples and electrically isolated from each other by standard photolithographic methods and an  $SF_6$  plasma etch. During these processes, the sample temperature never exceeded 90°C. Resistivity measurements were performed at room temperature, 77 and 4.2 K. The Hall effect was measured at 4.2 K in a magnetic field of up to 8 T.

X-ray-diffraction measurements confirmed that the  $Si(111):B-(\sqrt{3}\times\sqrt{3})R30^\circ/a$ -Si interface is present on these samples. The two-dimensional nature of the  $(\sqrt{3}\times\sqrt{3})R30^\circ$  reconstructed interface results in a two-dimensional lattice of x-ray-diffraction "rods" that are a

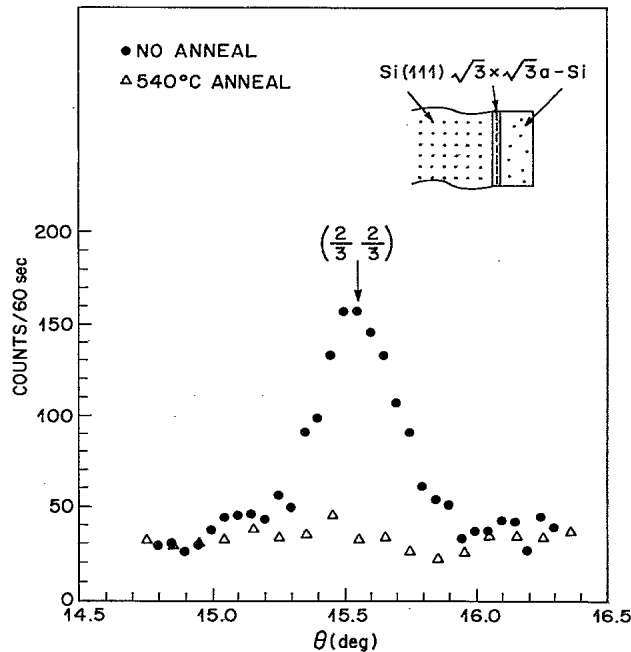


FIG. 2. Rocking scans through the  $(\frac{2}{3}, \frac{2}{3})$  surface x-ray-diffraction rod for the  $Si(111):B-(\sqrt{3}\times\sqrt{3})R30^\circ/a$ -Si reconstruction. The Si cap thickness was 50 Å. One sample was subsequently annealed at 540°C for 90 min before it was removed from the vacuum system.

slowly varying function of  $l$ , the momentum transfer perpendicular to the surface. The rods are indexed relative to the hexagonal  $Si(111)$  surface unit cell in the same way as LEED patterns are indexed.<sup>9</sup> Figure 2 shows rocking scans through the  $(\frac{2}{3}, \frac{2}{3})$  diffraction rod at  $l=0.2$ .

Secondary-ion mass spectroscopy was also performed on capped  $Si(111):B-(\sqrt{3}\times\sqrt{3})R30^\circ$  samples to investigate the localization of boron impurities perpendicular to the interface. Figure 3 shows a SIMS depth profile of a sample prepared by depositing boron at 700°C and capped with 200-Å  $a$ -Si. The FWHM of the profile is 50 Å and the integrated area under the profile corresponds to  $3.1\times 10^{14}$  cm<sup>-2</sup> boron. The resolution of the trailing edge of the profile is limited by the knock-on effect of the sputtering beam. For comparison, a depth profile for a sample held at the higher temperature of 800°C while boron was deposited is shown. This profile clearly shows a "tail" on the boron interface peak resulting from boron diffused into the crystal. The maximum concentration in the tail [obtained by subtracting profile (a) from (b)] is  $1\times 10^{20}$  cm<sup>-3</sup>; the solubility limit of boron in silicon. From further diffusion studies, we estimate that at 700°C,  $5\times 10^{13}$  cm<sup>-2</sup> boron diffuses into the crystal in 3 min with a diffusion length of  $\approx 35$  Å. This accounts for the difference between one-third of a monolayer of boron atoms ( $2.6\times 10^{14}$  cm<sup>-2</sup>) and the experimentally observed coverage ( $3.1\times 10^{14}$  cm<sup>-2</sup>). The boron impurity layer is thus confirmed to be ordered and almost completely confined to a single monolayer.

The resistance, magnetoresistance ( $\rho_{xx}$ ), and Hall effect ( $\rho_{xy}$ ) were measured on  $Si(111):B-(\sqrt{3}\times\sqrt{3})R30^\circ$  samples with various  $a$ -Si overlayer thicknesses. Capped  $B-(\sqrt{3}\times\sqrt{3})R30^\circ$  samples were conducting at room temperature, 77 and 4.2 K. From the Hall-effect measurement at 4.2 K, a  $p$ -type carrier density of  $(1.7-2.2)\times 10^{14}$  cm<sup>-2</sup> and a mobility of 25.9–36.6 cm<sup>2</sup>V<sup>-1</sup>s<sup>-1</sup> is obtained (Table I), indicating metallic behavior. No significant carrier freeze-out was observed upon cooling the samples. Since the mean separation between impuri-

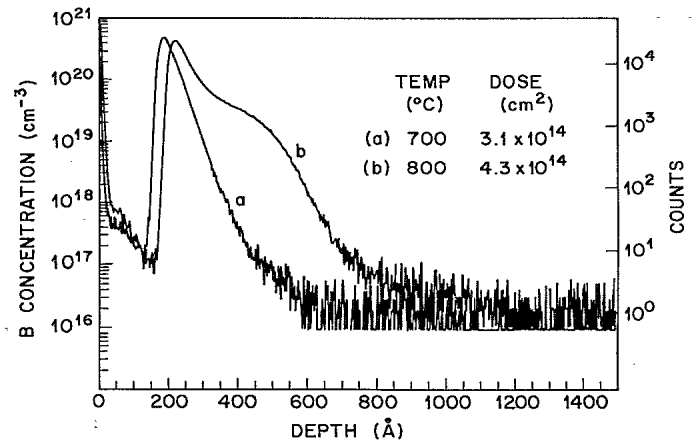


FIG. 3. SIMS profiles of boron  $(\sqrt{3}\times\sqrt{3})R30^\circ$   $n$ -type silicon at (a) 700°C and (b) at 800°C, with a 3-min exposure time. Both samples were covered with 200 Å of amorphous silicon.

TABLE I. 4.2-K Hall-effect results for Si(111)/*a*-Si interface reconstructions.

Reconstruction Initial	Reconstruction Final	<i>a</i> -Si thickness (Å)	$T_{\text{anneal}}$ (°C)	Boron coverage ( $10^{14} \text{ cm}^{-2}$ )		Carrier density ( $10^{14} \text{ cm}^{-2}$ )	Mobility ( $\text{cm}^2 \text{ V}^{-1} \text{ s}^{-1}$ )
				SIMS	NRA		
$(\sqrt{3} \times \sqrt{3})R 30^\circ$	$(\sqrt{3} \times \sqrt{3})R 30^\circ$	100	90	3.4	3.5	2.2	36.6
$(\sqrt{3} \times \sqrt{3})R 30^\circ$	$(\sqrt{3} \times \sqrt{3})R 30^\circ$	60	90	2.6	2.7	1.7	30.5
$(\sqrt{3} \times \sqrt{3})R 30^\circ$	$(\sqrt{3} \times \sqrt{3})R 30^\circ$	50	90	3.1	3.4	1.8	25.9
$(\sqrt{3} \times \sqrt{3})R 30^\circ$	Disordered	100	700	3.4	3.5	3.2	47.9
$(\sqrt{3} \times \sqrt{3})R 30^\circ$	Disordered	0	90	3.1	3.4	0	
$(\sqrt{3} \times \sqrt{3})R 30^\circ$	Disordered	60	500	2.6	2.7	2.4	31.9
7×7	7×7	50	90	0.1		0	

ties, 6.7 Å, is smaller than the effective Bohr radius for heavy holes in silicon ( $\approx 13$  Å), we might naively expect the  $(\sqrt{3} \times \sqrt{3})R 30^\circ$  interface to be metallic. On the other hand, as a consequence of Bloch's theorem, the ordered two-dimensional impurity layer generates a new band structure which could, in principle, result in a nonconducting layer. The magnetoresistance was less than 2% up to 8 T which was too small to determine its dependence on the orientation of the magnetic field. Shubnikov-de Haas (SdH) oscillations were not observed on any of the samples. SdH oscillations are not expected by the following argument: Assuming a heavy-hole effective mass of  $m_{\text{hh}}^* = 0.49m_0$ , the ratio of the cyclotron frequency  $\omega_c$  to the scattering rate  $\tau^{-1}$  is found to be  $\omega_c \tau \approx 0.03$  at a field of 8 T, so the condition  $\omega_c \tau \gg 1$  to observe the Shubnikov-de Haas effect is not fulfilled.

Annealing Si(111):B- $(\sqrt{3} \times \sqrt{3})R 30^\circ/a$ -Si samples at 500°C–700°C prior to defining the bridge structure causes the *a*-Si layer to recrystallize, the  $(\sqrt{3} \times \sqrt{3})R 30^\circ$  structure to become disordered (Fig. 2), and increases the electrically active carrier density by  $0.7$ – $1.0 \times 10^{14} \text{ cm}^{-2}$  (Table I). The increase in carrier density upon annealing may be caused by the removal of defects such as boron interstitials in the impurity layer or traps associated with the amorphous-silicon layer. For example, vapor-deposited amorphous silicon contains  $\approx 10^{20} \text{ cm}^{-3}$  states distributed nearly uniformly over the forbidden band;<sup>11</sup> these states pin the Fermi level near the center of the band gap.<sup>12</sup> By application of Poisson's equation, we calculate  $0.3 \times 10^{14} \text{ cm}^{-2}$  space charge in the depletion region between B- $(\sqrt{3} \times \sqrt{3})R 30^\circ$  and amorphous silicon. These states are removed by recrystallization of the *a*-Si, and hence the measured carrier density is larger after annealing.

The same measurements discussed above were also performed for several control samples such as B- $(\sqrt{3} \times \sqrt{3})R 30^\circ$  samples not capped with *a*-Si before removal from the vacuum system, and the buried 7×7 interface structure with no intentional boron. Neither of these samples were conducting at 4.2 K (Table I).

When the boron  $(\sqrt{3} \times \sqrt{3})R 30^\circ$  samples are not capped with *a*-Si and exposed to air, the surface reconstruction is consumed by the native oxide, removing any conducting surface states. We know that the room-temperature oxidation of the surface is very slow since the  $(\sqrt{3} \times \sqrt{3})R 30^\circ$  reconstruction is still observed on uncapped samples for several hours during exposure to air

at atmospheric pressure. This sample then provides another measure of the boron diffused into the bulk during growth. Boron diffused in more than  $\approx 10$  Å should still be electrically active even on the uncapped samples. Since the uncapped samples were nonconducting at 4.2 K, and it is known that freeze-out occurs for concentrations of  $\lesssim 10^{18} \text{ cm}^{-3}$ , the concentration of diffused boron is negligible compared to the surface boron concentration. In addition, the buried 7×7 samples did not conduct at 4.2 K, thus conduction through the *n*-type substrate is ruled out. Auger measurements during sample growth show that boron does not segregate into the *a*-Si layer, so the *a*-Si also remains nonconducting. We conclude that the observed carrier concentration in Si(111):B- $(\sqrt{3} \times \sqrt{3})R 30^\circ$  samples can only be explained by conductivity in the ordered impurity layer.

The 7×7 reconstructed surface of Si(111) has a high density of surface states in the band gap of Si.<sup>13,14</sup> Surface-conductivity measurements in ultrahigh vacuum show that the 7×7 surface is conducting.<sup>15</sup> However, the buried Si(111)-7×7 does not show conductivity at 4.2 K (see Table I). In Ref. 13 it was found that the high density of states just above the valence-band edge can be attributed predominantly to the dangling bond on Si adatoms. The density of these states is therefore as large as the density of adatoms on the surface, or 12 per 7×7 unit cell ( $1.9 \times 10^{14} \text{ cm}^{-2}$ ), and since the dangling-bond states are half-full they are expected to be metallic. Several studies have shown that Si adatoms on the 7×7 and on the B- $(\sqrt{3} \times \sqrt{3})R 30^\circ$  are removed from ordered sites by the addition of amorphous silicon.<sup>1,8,9</sup> This suggests that there is an interaction between the crystal surface and the amorphous layer in which new chemical bonds are formed. The amorphous-silicon layer passivates nearly all of the surface dangling bonds so that surface states are no longer present at the Si(111)-7×7/*a*-Si interface.

In contrast to the 7×7 reconstruction, the B- $(\sqrt{3} \times \sqrt{3})R 30^\circ$  surface has been found to be semiconducting with a band gap comparable to bulk silicon.<sup>2,3,16</sup> On the B- $(\sqrt{3} \times \sqrt{3})R 30^\circ$  surface, the electron in the dangling-bond state is transferred to a subsurface boron atom. The result is that the dangling-bond state is completely empty, and therefore, nonconducting.<sup>16</sup> The boron layer is also nonconducting; since there is exactly one dangling-bond state per boron atom on the B- $(\sqrt{3} \times \sqrt{3})R 30^\circ$  surface, the transfer of electrons from the surface depletes the layer completely.

The present results show that capping this surface with amorphous silicon results in a fundamental change in the nature of the reconstruction from a nonconducting layer to a conducting (metallic) layer. Thus, when the dangling-bond states are passivated by amorphous silicon, the  $p$ -type carriers return to conducting states and a metallic layer with the observed high  $p$ -type carrier density is created.

The two-dimensional mean free path,  $\hbar\mu/e(2\pi p)^{1/2}$ , corresponding to the measured mobility  $\mu$  of  $37 \text{ cm}^2 \text{ V}^{-1} \text{ s}^{-1}$  is  $90 \text{ \AA}$ ; where  $p$  is the carrier concentration. This is 14 times larger than the impurity spacing of  $6.7 \text{ \AA}$  in the  $(\sqrt{3} \times \sqrt{3})R 30^\circ$  reconstruction. A mean impurity spacing of  $6.7 \text{ \AA}$  corresponds to a bulk concentration of  $3.3 \times 10^{21} \text{ cm}^{-3}$  (this is 7% of the atomic density of crystalline silicon). The mobility in this case is only  $17 \text{ cm}^2 \text{ V}^{-1} \text{ s}^{-1}$  (Ref. 17), and the corresponding mean free path is  $50 \text{ \AA}$ . There are several phenomena which may account for the large mobility and mean free path in the interface reconstruction compared to bulk silicon: (1) When the two-dimensional impurity layer is narrower than the carrier wave function ( $13 \text{ \AA}$ ), the carriers spend less time in the vicinity of the ionized impurity than in the case of bulk impurities with the same mean carrier separation.<sup>18</sup> (2) An ordered impurity layer should have a lower elastic scattering rate than a corresponding disordered layer.<sup>19</sup> (3) The heavy-hole effective mass,  $m_{hh}^*$ , may be smaller in the two-dimensional band structure than in bulk silicon.

Electrical activity in semiconductors is typically

achieved by introducing a low density of  $n$ - or  $p$ -type substitutional impurities into the host material. Since the average separation between impurities is large (in the range  $50\text{--}1000 \text{ \AA}$ ) compared to the lattice constant of the host material (around  $5 \text{ \AA}$ ) the spatial distribution of impurities is usually assumed to be random. However, at very high concentrations ( $> 10^{21} \text{ cm}^{-3}$ ) the fact that substitutional impurities only occupy discrete lattice sites gives rise to spatial correlation effects, so a description in terms of a continuous random spatial distribution function is no longer correct. Very high impurity concentrations are difficult to achieve in bulk material. However, we have shown that it is possible to create two-dimensional structures involving high concentrations of impurity atoms that are *completely ordered*. Such structures may exhibit useful and interesting new electrical phenomena because of correlation effects.

In conclusion, we have demonstrated an ordered two-dimensional impurity layer with an exceptionally high  $p$ -type carrier density at the  $\text{Si}(111)\text{:B-}(\sqrt{3} \times \sqrt{3})R 30^\circ/a\text{-Si}$  interface. The SIMS profile, x-ray-diffraction measurement, and Hall-effect measurement show that the boron layer is ordered in a single monolayer at the interface and electrically active with a mobility greater than the corresponding bulk value. The electrical activity is attributed to passivation of surface states by the  $a\text{-Si}$  layer.

We thank I. K. Robinson, J. E. Rowe, E. F. Schubert, F. Schrey, R. T. Tung, E. Vlieg, and B. E. Weir for valuable contributions.

- 
- <sup>1</sup>R. L. Headrick, I. K. Robinson, E. Vlieg, and L. C. Feldman, *Phys. Rev. Lett.* **63**, 1253 (1989).
- <sup>2</sup>P. Bedrossian, R. D. Meade, K. Mortensen, D. M. Chen, J. A. Golovchenko, and D. Vanderbilt, *Phys. Rev. Lett.* **63**, 1257 (1989).
- <sup>3</sup>I.-W. Lyo, E. Kaxiras, and Ph. Avouris, *Phys. Rev. Lett.* **63**, 1261 (1989).
- <sup>4</sup>R. L. Headrick, L. C. Feldman, and I. K. Robinson, *Appl. Phys. Lett.* **55**, 442 (1989).
- <sup>5</sup>K. Akimoto, J. Mizuki, I. Hirose, T. Tatsumi, H. Hirayama, N. Aizaki, and J. Mizuki, *Extended Abstracts of the 19th Conference on Solid State Devices and Materials* (Business Center for Academic Societies, Tokyo, 1987).
- <sup>6</sup>M. Tabe, *Jpn. J. Appl. Phys.* **21**, 534 (1982).
- <sup>7</sup>M. P. Seah and W. A. Dench, *Surf. Int. Anal.* **1**, 2 (1979).
- <sup>8</sup>J. M. Gibson, H. -J. Gossmann, J. C. Bean, R. T. Tung, and L. C. Feldman, *Phys. Rev. Lett.* **56**, 355 (1986).
- <sup>9</sup>I. K. Robinson, W. K. Waskiewicz, R. T. Tung, and J. Bohr, *Phys. Rev. Lett.* **57**, 2714 (1986).
- <sup>10</sup>L. C. Feldman and S. T. Picraux, in *Ion Beam Handbook for Materials Analysis*, edited by J. W. Mayer and E. Rimini (Academic, New York, 1977), p. 112.
- <sup>11</sup>K. Seeger, *Semiconductor Physics* (Springer-Verlag, New York, 1982).
- <sup>12</sup>W. A. Harrison, *Solid State Theory* (Dover, New York, 1979); M. H. Cohen, H. Fritzsche, and S. R. Ovshinsky, *Phys. Rev. Lett.* **22**, 1065 (1969).
- <sup>13</sup>R. J. Hamers, R. M. Tromp, and J. E. Demuth, *Phys. Rev. Lett.* **56**, 1972 (1986).
- <sup>14</sup>F. J. Himpsel and Th. Fauster, *J. Vac. Sci. Technol. A* **2**, 815 (1984).
- <sup>15</sup>F. Bäuerle, W. Mönch, and M. Henzler, *J. Appl. Phys.* **43**, 3917 (1972).
- <sup>16</sup>E. Kaxiras, K. C. Pandey, F. J. Himpsel, and R. M. Tromp, *Phys. Rev. Lett.* **64**, 551 (1990).
- <sup>17</sup>G. Masetti, M. Severi, and S. Solmi, *IEEE Trans. Electron. Devices* **30**, 764 (1983).
- <sup>18</sup>E. F. Schubert, J. E. Cunningham, and W. T. Tsang, *Solid State Commun.* **63**, 591 (1987).
- <sup>19</sup>A. F. J. Levi, S. L. McCall, and P. M. Platzman, *Appl. Phys. Lett.* **54**, 940 (1989).